

Effect of Cobalt on the Magnetic Properties of the $\text{LiFe}_{1-x}\text{Co}_x\text{O}_2$ Layered System ($0 \leq x \leq 1$)

E. Chappel,* M. Holzapfel,^{†,‡} G. Chouteau,* and A. Ott[‡]

* Grenoble High Magnetic Field Laboratory, CNRS and MPI-FKF, 25 avenue des Martyrs, BP 166, 38042 Grenoble Cedex 9, France;

[†] Laboratoire d'Electrochimie et de Physicochimie des Matériaux et des Interfaces, ENSEEG, INPG, 1130, rue de la piscine, BP 75, 38402 St. Martin d'Hères, France; and [‡] Institut für Anorganische Chemie, Universität Tübingen, Auf der Morgenstelle 18, 72070, Tübingen, Germany

Received March 14, 2000; in revised form June 13, 2000; accepted July 13, 2000; published online September 30, 2000

Layered $\text{LiFe}_{1-x}\text{Co}_x\text{O}_2$ was prepared in the whole composition range by ion-exchange reaction in a molten eutectic mixture of LiCl and LiNO_3 at 260°C . The magnetic properties were studied by means of magnetic susceptibility and high-field magnetization measurements. Layered LiFeO_2 exhibits a Néel temperature of $T_N = 20$ K. Some cationic disorder is present but seems to have no effect on the magnetic properties. The saturation magnetization and the number of effective Bohr magnetons are consistent with the high spin state ($S = \frac{5}{2}$) of the Fe^{3+} ion. A two sublattice model consisting of antiferromagnetic order between ferromagnetic layers is proposed with an estimation of the ferro- and antiferromagnetic interactions. Replacing iron by cobalt leads to an increase of the Weiss temperature θ up to $x = 0.4$ but at the same time the antiferromagnetic long-range order is destroyed. The effect of cobalt on the superexchange interactions is also discussed. © 2000 Academic Press

Key Words: magnetic oxides; metamagnetism; mean field model; high magnetic fields.

I. INTRODUCTION

AMO_2 layered oxides ($A = \text{Li, Na}$ and $M = 3d$ element) have been intensively studied for utilization as positive electrode materials in high-energy density batteries (1–4). LiFeO_2 with the $\alpha\text{-NaFeO}_2$ type structure (denoted as layered LiFeO_2) would be an attractive alternative to LiNiO_2 and LiCoO_2 as it is cheaper and nontoxic. However, it is not fully understood why the layered LiFeO_2 obtained by ion-exchange reaction is not electrochemically active (5–9). Layered LiFeO_2 crystallizes in the $R\bar{3}m$ space group which can also be described as a packing of FeO_2 and LiO_2 slabs built up of edge-sharing FeO_6 (LiO_6) octahedra to form a triangular Fe (Li) lattice. We have undertaken a systematic study of the $\text{LiFe}_{1-x}\text{Co}_x\text{O}_2$ ($0 \leq x \leq 1$) solid solution. The initial idea was that the presence of some cobalt in layered LiFeO_2 would have the same effect as in $\text{LiNi}_{1-x}\text{Co}_x\text{O}_2$: reducing the amount of $3d$ metals in the

lithium site would lead to easier lithium diffusion during the intercalation/deintercalation process (10). The physical properties of such systems strongly depend on the nature of the chemical bonding within the MO_2 slabs. Recently, several experimental studies have been done on isomorphous $\text{Li}_{1-x}\text{Ni}_{1+x}\text{O}_2$ (11, 12). While a cooperative Jahn–Teller effect is observed in magnetically ordered NaNiO_2 , its absence in $\text{Li}_{1-x}\text{Ni}_{1+x}\text{O}_2$ is very puzzling (15). The presence of a spin orbital liquid has been recently proposed, as a consequence of quantum fluctuations between degenerate classical configurations (13), or simply due to the frustration of the triangular lattice preventing a staggered orbital ordering for the degenerate e_g states (14). Only a few works have been devoted to the layered LiFeO_2 (9, 16, 17) and $\text{LiFe}_{1-x}\text{Co}_x\text{O}_2$ (18). Here we report a complete study of the static magnetic properties of the $\text{LiFe}_{1-x}\text{Co}_x\text{O}_2$ series in the whole composition range. From very high field magnetization analysis, an A -type antiferromagnetic structure is proposed for layered LiFeO_2 in striking analogy with NaNiO_2 (12, 19). The signs and the values of the inter- and intralayer magnetic interactions are also discussed. We show that cobalt ions essentially fit in the $3d$ planes, increasing the Weiss temperature up to $x = 0.4$. This effect was also observed in the $\text{Li}_{1-x}\text{Ni}_{1+x}\text{O}_2$ and NaNiO_2 systems (20, 21). It is accompanied by the gradual destruction of the long-range antiferromagnetic order. For $x > 0.4$ only short-range ferromagnetic in-plane interactions remain. Analysis of these results allows us to establish the effect of the cobalt ions on the magnetic properties of $\text{LiFe}_{1-x}\text{Co}_x\text{O}_2$.

II. EXPERIMENTAL

Synthesis of the members of the series $\text{LiFe}_{1-x}\text{Co}_x\text{O}_2$ was achieved through ion-exchange reaction starting from $\text{NaFe}_{1-x}\text{Co}_x\text{O}_2$. As starting materials Na_2O_2 powder (95%, Fluka), Co_3O_4 (puriss. P. A., Merck) and Fe_2O_3 (carbonyl iron oxide, BASF) were thoroughly mixed with a slight excess of Na_2O_2 is an agate mortar under an argon

atmosphere. The powders were heated in air in corundum boats with intermittent grinding and analyzed by X-ray diffraction (XRD, Philips powder diffractometer PW1130/00, Ni-filtered $\text{CuK}\alpha$ radiation, Au standard).

The different members of the $\text{LiFe}_{1-x}\text{Co}_x\text{O}_2$ series were obtained by reacting the $\text{NaFe}_{1-x}\text{Co}_x\text{O}_2$ samples in an eutectic LiCl/LiNO_3 mixture for 6 h (molar ratio sodium compound vs lithium salt 1 : 10), washed with methanol, and dried in vacuum. More details are given elsewhere (10).

Profile refinements were performed by Rietveld analysis using the program FULLPROF 90 (22) based on diffraction patterns obtained on a Philips PW 1830 diffractometer for $15^\circ \leq 2\theta \leq 90^\circ$.

Magnetic susceptibility measurements were performed using a SQUID magnetometer (Quantum Design, MPMS) at 1 kOe between 4 and 200 K and an extraction magnetometer up to 600 kOe at 20 kOe. High magnetic field measurements (up to 230 kOe) were performed at Grenoble High Magnetic Field Laboratory facilities using resistive magnets.

III. RESULTS AND DISCUSSION

A. X-Ray Diffraction and Structure Refinements

Single-phase products were obtained according to the XRD results shown in Fig. 1. Only in the case of $\text{LiFe}_{0.8}\text{Co}_{0.2}\text{O}_2$ are traces of a second phase (less than 5%) visible as two additional reflections at $2\theta = 18.95^\circ$ and $2\theta = 45.25^\circ$ (probably LiCoO_2). The real concentration of the latter sample would be also written $\text{LiFe}_{0.85}\text{Co}_{0.15}\text{O}_2$. Chemical analysis by AAS measurements and a determination of the mean oxidation number of the transition metal ions are described in (10).

The $\text{LiFe}_{1-x}\text{Co}_x\text{O}_2$ compounds crystallize in the α - NaFeO_2 structure. The lattice constants decrease with the

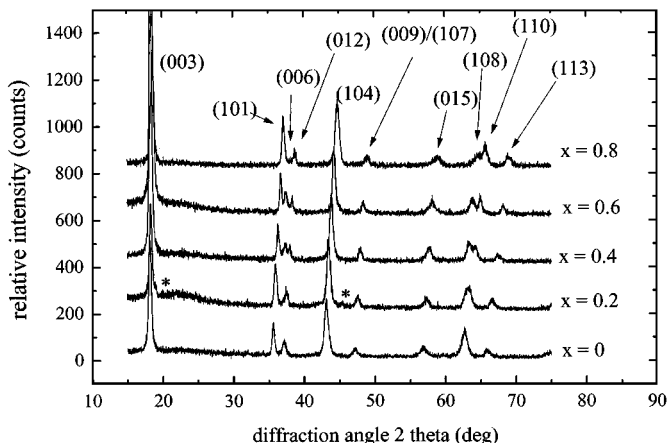


FIG. 1. XRD diagrams for several compounds of the system $\text{LiFe}_{1-x}\text{Co}_x\text{O}_2$. The spectra are shifted along the y axis for clarity. Asterisks denote peaks resulting from LiCoO_2 impurity.

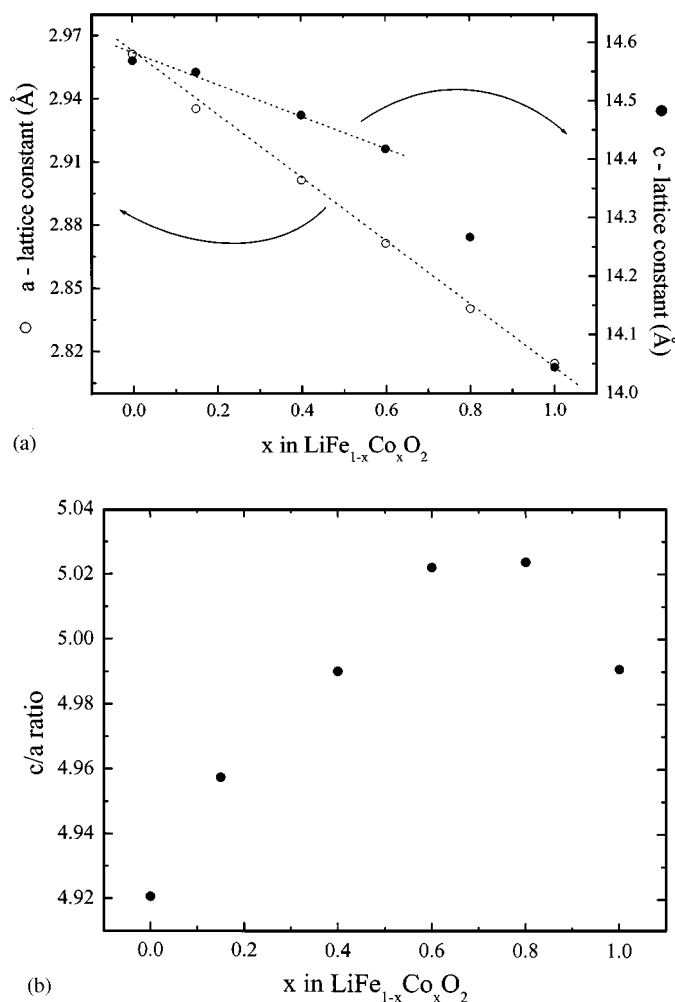


FIG. 2. Hexagonal lattice constants (a) and c/a ratio (b) for $\text{LiFe}_{1-x}\text{Co}_x\text{O}_2$ as a function of the composition x . Open circles denote the a constant, solid circles the c constant. The dashed lines denote the linear behavior for the lattice constants (linear only for $0 \leq x \leq 0.6$ for the c constant).

cobalt concentration (Fig. 2a). For the a constant a linear behavior is observed whereas for the c value, and consequently for the c/a ratio (Fig. 2b), strong deviation from this behavior occur.

The increase of the c lattice constant is bigger than expected for a simple substitution of Fe^{3+} by Co^{3+} . Assuming a partial disorder of M^{3+} in the $3a$ sites (almost perfect cationic order is known for LiCoO_2 ; thus Fe^{3+} is assumed to be disordered, but XRD-Rietveld analysis does not allow a clear distinction between Fe^{3+} and Co^{3+}) implies a partial occupation of the $3b$ positions by lithium. The bigger ionic radius of Li^+ (23) in comparison with Fe^{3+} and Co^{3+} causes an inflation of the MO_2 layers and thus an enhanced c value. Assuming that below $x = 0.6$ the disorder does not increase, only cobalt substitution for iron in $3b$ is responsible for the change of the c lattice parameter between

TABLE 1
Results of the Profile Refinements on $\text{LiCo}_{0.6}\text{Fe}_{0.4}\text{O}_2$ and LiFeO_2

Atom	Position	Occupation	x	y	z	
$\text{LiCo}_{0.6}\text{Fe}_{0.4}\text{O}_2$						
Li	3a	0.955(3)	0	0	0	$a = 2.857(3) \text{ \AA}; c = 14.355(9) \text{ \AA}$
Li	3b	0.045(3)	0	0	0.5	$B = 0.555 \text{ \AA}^2$
Fe/Co	3a	0.045(3)	0	0	0	$R_p = 7.27; R_{wp} = 9.46$
Fe/Co	3b	0.955(3)	0	0	0.5	$R_{\text{Bragg}} = 6.23$
O	6c	1.000	0	0	0.2391(5)	$R_f = 7.38$
LiFeO_2						
Li	3a	0.954(2)	0	0	0	$a = 2.950(3) \text{ \AA}; c = 14.533(7) \text{ \AA}$
Li	3b	0.046(2)	0	0	0.5	$B = 0.645 \text{ \AA}^2$
Fe	3a	0.046(2)	0	0	0	$R_p = 9.22; R_{wp} = 12.8$
Fe	3b	0.954(2)	0	0	0.5	$R_{\text{Bragg}} = 3.46$
O	6c	1.000	0	0	0.2433(4)	$R_f = 3.50$

$x = 0.6$ and LiFeO_2 ($x = 0$). For $0 \leq x \leq 0.6$, the linear increase is thus less steep than for $0.6 \leq x \leq 1$, where both effects, the substitution and the increasing disorder, are present. Hence, the XRD results are consistent with a partial disorder of Fe^{3+} in 3a sites. At $x \approx 0.6$ it is comparable to the disorder observed in LiFeO_2 .

This result is supported by Rietveld analysis performed for LiFeO_2 and $\text{LiFe}_{0.4}\text{Co}_{0.6}\text{O}_2$ using FULLPROF 90 which is described in more detail in (10).

The results of the refinement are shown in Table 1 and the observed and calculated diffraction for LiFeO_2 and $\text{LiFe}_{0.4}\text{Co}_{0.6}\text{O}_2$ patterns in Fig. 3. They indicate that the assumption of $\alpha\text{-NaFeO}_2$ type for the series $\text{LiFe}_{1-x}\text{Co}_x\text{O}_2$ is correct. LiFeO_2 shows a cationic disorder of 4.5%. For $\text{LiFe}_{0.4}\text{Co}_{0.6}\text{O}_2$ 4.5% was calculated too, in agreement with the above-mentioned appreciable disorder already present for relatively low iron contents.

B. Magnetic Properties

In Fig. 4 the temperature dependence of M/H is reported for $\text{LiFe}_{1-x}\text{Co}_x\text{O}_2$ with $x = 0$ (Fig. 4a) and $x = 0.15, 0.4, 0.6$, and 0.8 (Fig. 4b). If we define the Néel temperature T_N as the maximum of the $M/H(T)$ curve, we find $T_N \simeq 20, 19$, and 8 K for $x = 0, 0.15$, and 0.4 , respectively. The two other samples ($x = 0.6$ and 0.8) do not show any long-range order above 4 K but short-range correlations are evidenced by the departure from the linear law of H/M at low temperature (see Fig. 5a). The M/H vs T curve of the $x = 0.4$ sample shows a second slight cusp around 16 K which could be attributed to some inhomogeneities of the in-plane Fe/Co cationic distribution. The temperature dependence of H/M in the high-temperature regime ($300 \text{ K} < T < 600 \text{ K}$) given in Fig. 5b obeys the Curie-Weiss law

$$\chi^{-1} = \frac{T - \theta}{C}, \quad [1]$$

where C is the Curie constant. We observe a positive Weiss temperature θ for all samples, which indicates the presence of dominant ferromagnetic interactions. We deduce from

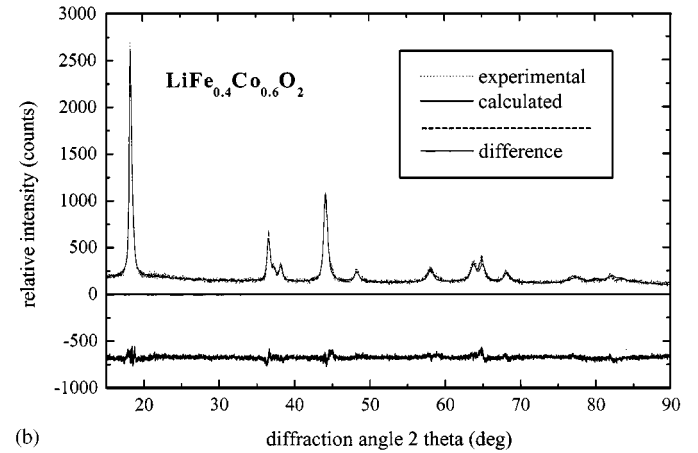
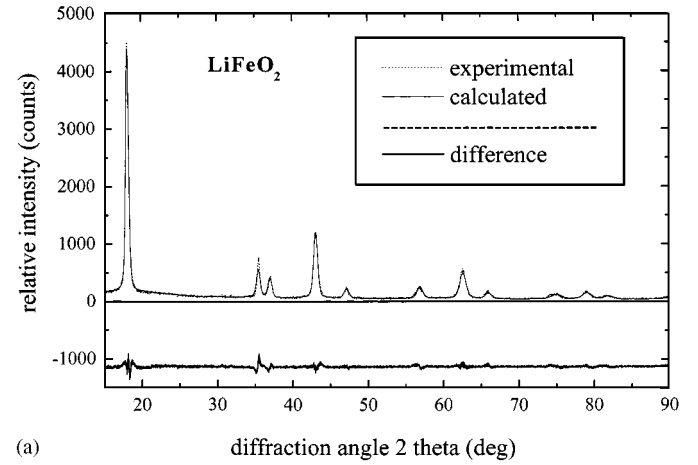


FIG. 3. Calculated and observed X-ray diffraction profiles for the series (a) LiFeO_2 and (b) $\text{LiFe}_{0.4}\text{Co}_{0.6}\text{O}_2$.

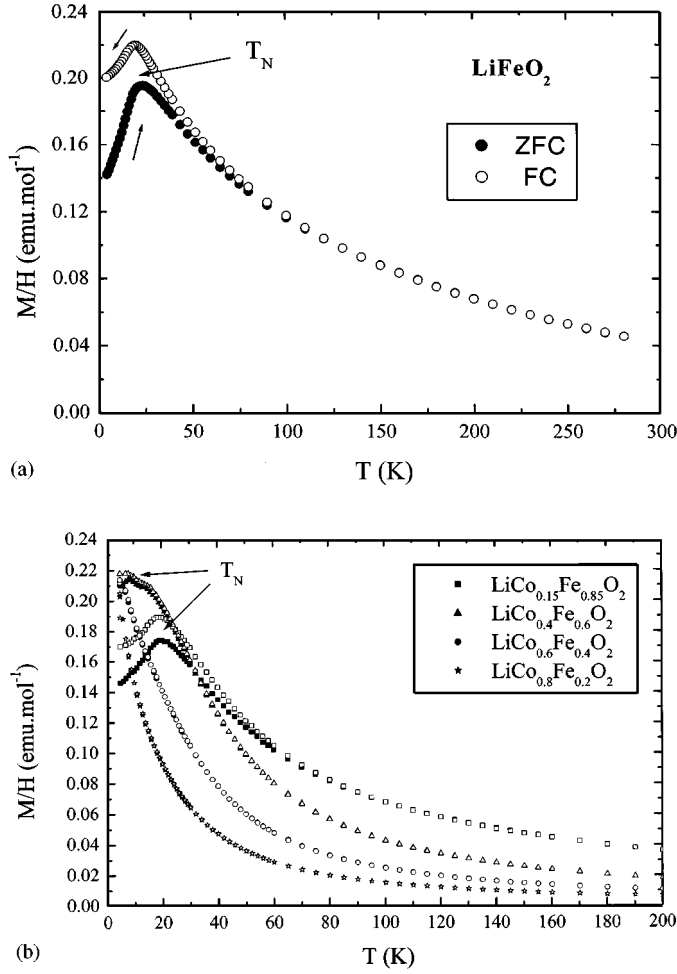


FIG. 4. Temperature dependence of M/H at $H = 1$ kOe for layered LiFeO_2 (a) and for $\text{LiFe}_{1-x}\text{Co}_x\text{O}_2$ with $x = 0.15, 0.4, 0.6$, and 0.8 (b). The open and solid marks correspond to measurements on field cooling and on heating after zero-field cooling, respectively.

this data the Curie constant and the effective Bohr magneton number

$$\frac{\mu_{\text{eff}}}{\mu_B} = \left(\frac{3kC}{N_A \mu_B^2} \right)^{1/2} \quad [2]$$

where k is the Boltzmann constant and N_A Avogadro's number. Assuming Fe^{3+} ion in the high-spin state ($t_{2g}^3 e_g^2$) with $S = \frac{5}{2}$ (16) and Co^{3+} ion in the low-spin state ($t_{2g}^6 e_g^0$) with $S = 0$ (18), we find a good agreement with the spin-only values (Fig. 6). In Fig. 7 the theoretical magnetization curves of a metamagnetic system at low temperature with strong (a) or weak (b) magnetic anisotropy are shown (24). These curves will be discussed in more detail later. Figure 8 represents the temperature dependence of M/H for layered LiFeO_2 under various magnetic fields. We observe a metamagnetic transition around $H_{\text{SF}} = 65$ kOe for layered

LiFeO_2 as is evidenced by a constant value for M/H below the transition temperature. For $H > H_{\text{SF}}$ and $T < T_N$ the susceptibility is actually constant to a first approximation since all spins are in a transverse configuration. In Fig. 9 we report very high field magnetization measurements for all samples. The magnetization at constant temperature exhibits a change of slope at the phase transition field as expected. Magnetic saturation is almost reached for all samples: the experimental values are in good agreement with the high-spin state of iron (Fig. 6b). We obtain exactly the expected values except for LiFeO_2 . In this compound, the magnetic susceptibility measurement indicates a small excess of spin ($\mu_{\text{eff}}/\mu_B = 6.03$ instead of 5.91 for the pure compound). Crystallographic data reveal a small fraction of iron in the Li site. This could create an antiferromagnetic

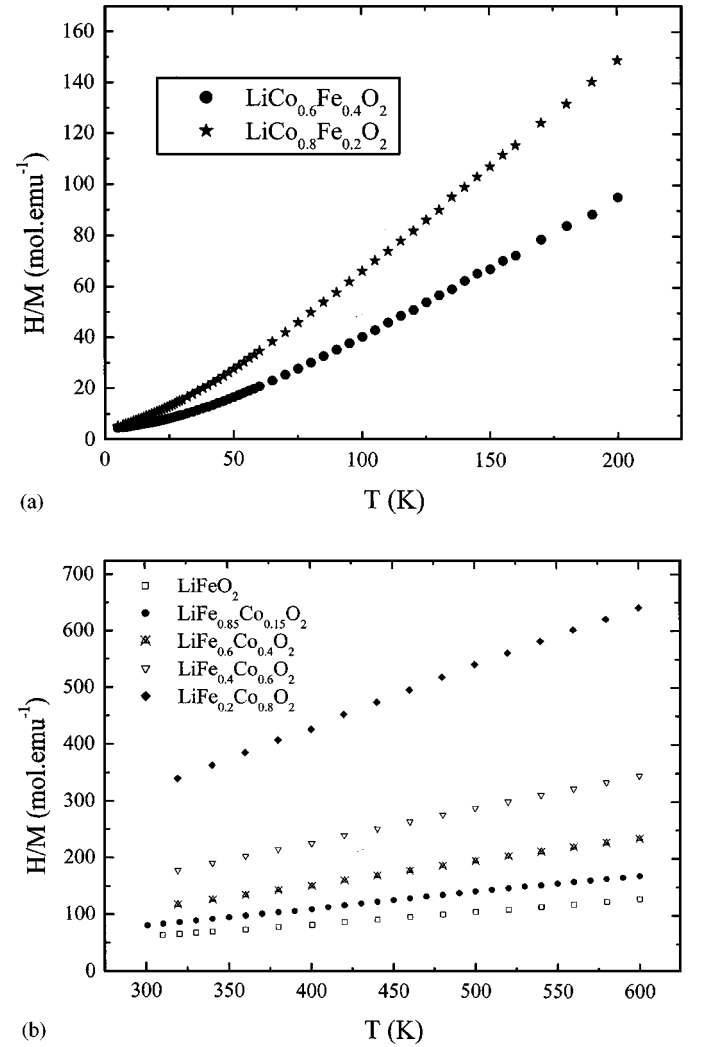


FIG. 5. Temperature dependence of H/M at $H = 1$ kOe for $\text{LiFe}_{1-x}\text{Co}_x\text{O}_2$ with $x = 0.6$ and 0.8 (a) and at $H = 20$ kOe for all samples in the high-temperature regime (b). These data fit very well with a straight line derived from the Curie-Weiss law.

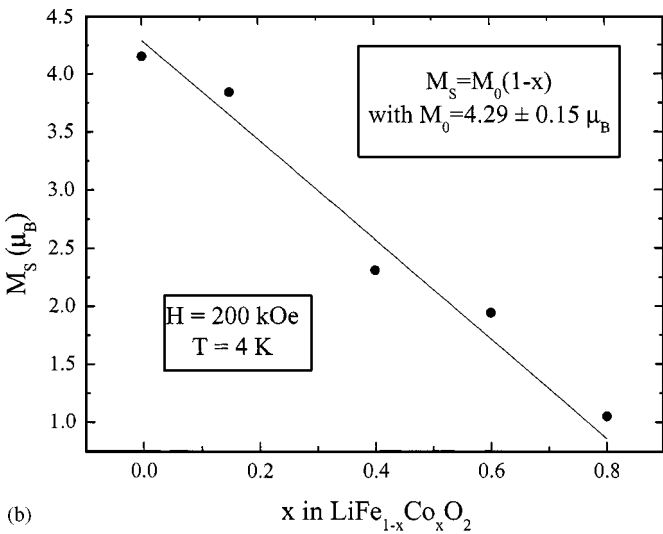
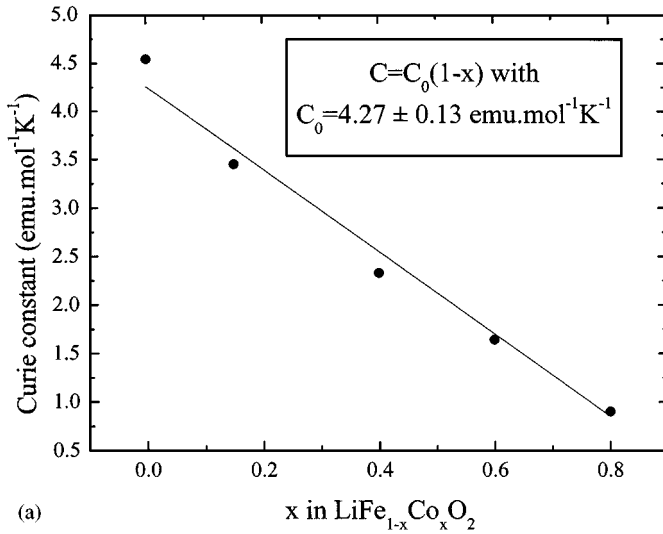


FIG. 6. (a) Curie constant derived from high-temperature magnetization measurements ($300 \text{ K} < T < 600 \text{ K}$) and (b) magnetization at saturation obtained at 200 kOe for $\text{LiFe}_{1-x}\text{Co}_x\text{O}_2$ series. The linear law observed directly proves the absence of clusters (11, 15).

interaction at 180° as in $\text{Li}_{1-x}\text{Ni}_{1+x}\text{O}_2$ (11, 15). For the other samples, the mixing between iron and cobalt reduces this effect. We cannot exclude the presence of a small amount of cubic phase or of Fe^{3+} ions in the tetrahedral site for LiFeO_2 to explain the discrepancy in the magnetization. Nevertheless, the Fe^{3+} ions in the Li site seem to be less efficient to create a ferrimagnetic cluster than Ni^{2+} in $\text{Li}_{1-x}\text{Ni}_{1+x}\text{O}_2$ because no evidence of ferromagnetism is observed in the magnetization curve (15) and moreover the Curie constant C and the magnetization at saturation M_s follow exactly the linear laws $C = C_0(1-x)$ and $M_s = M_0(1-x)$ (Fig. 6a and 6b). We do not observe any spontaneous magnetization, a signature of such clusters or

of small amounts of impurities like Fe_3O_4 or $\gamma\text{-Fe}_2\text{O}_3$ (5, 11).

C. Discussion

The Goodenough–Kanamori–Anderson rules can give us an idea of the magnetic interactions expected in layered LiFeO_2 , even if the d^5 case is not favorable for theoretical predictions. We will next compare these predictions with our experimental results.

In the FeO_2 slabs there are only 90° bonds (Fe-O-Fe) while between the slabs only 180° bonds take place via oxygen. Among the great many potential exchange terms in the d^5 case, the $d_{z^2}-d_{z^2}$ AF contribution between two Fe^{3+} ions in the 180° exchange must be dominant (25). Also if the conditions of the semicovalency model are satisfied (26, 27), the virtual excitations between full O 2p orbitals and empty Fe^{3+} hybrid orbitals will produce again an AF exchange interaction (29, 30). Nevertheless, the ferromagnetic components of the 180° exchange in the d^5 case cannot be neglected and this will strongly reduces the value of the effective AF interaction compared with the case of Ni^{3+} ($3d^7$, $S = \frac{1}{2}$) with full t_g^2 orbitals. One can explain in this way the absence of

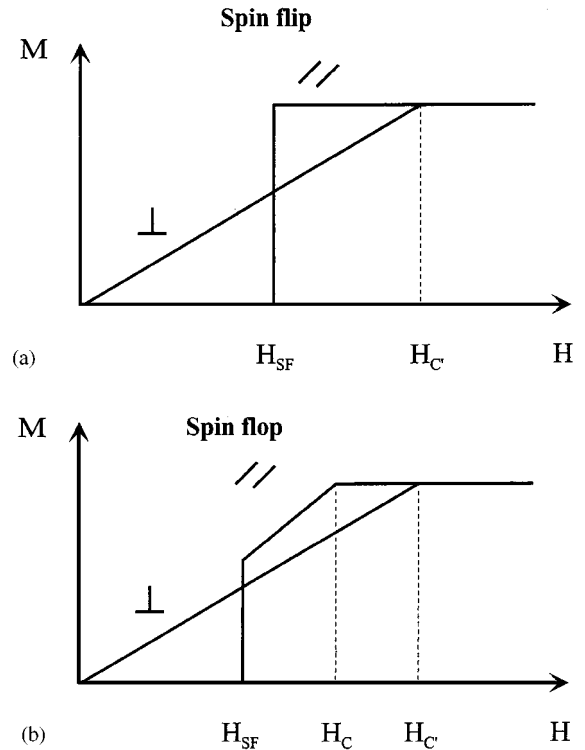


FIG. 7. Theoretical magnetization curves of a metamagnet at low temperature with strong (a) or weak (b) anisotropy. H_{SF} is the value of the spin flip (a) and spin flop (b) field extrapolated to 0 K; H_C and H'_C are the critical fields extrapolated to 0 K for the parallel and perpendicular cases, respectively.

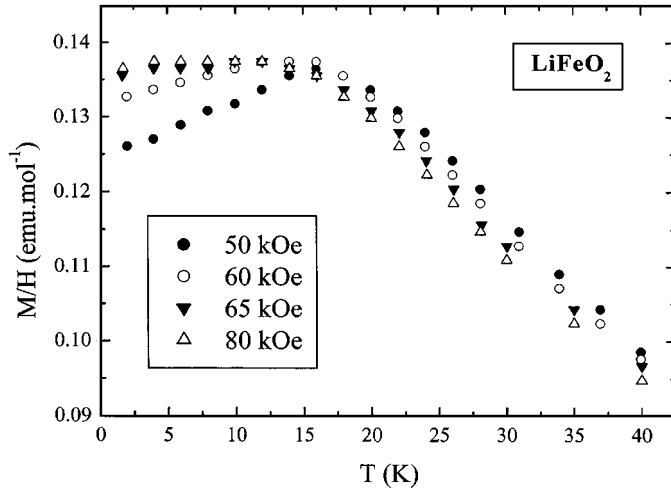


FIG. 8. Temperature dependence of H/M at different magnetic fields for layered LiFeO_2 . The spin flop field is estimated as $H_{\text{SF}} = 65 \text{ kOe}$. For $H > H_{\text{SF}}$ and $T < T_N$ the susceptibility is actually constant to a first approximation.

ferrimagnetic clusters. The intralayer interactions between Fe^{3+} at 90° should be weak and can be in principle F or AF: AF is expected from the interaction of the d_{xz} orbital of one cation with d_{z^2} and $d_{x^2-y^2}$ orbitals of the other, but F from the interaction of same orbitals on both cations. Since the virtual excitations involve orthogonal O 2p orbitals, Hund's rule acting on oxygen will also favor ferromagnetism in the latter case. Ferromagnetism is in fact often observed.

Let us first focus on the layered LiFeO_2 compound. The magnetization curve and the positive Curie-Weiss temperature suggest a two-sublattice model with ferromagnetic interaction in the layers and antiferromagnetic interaction between the layers. Using the molecular field theory and taking H_E as the exchange field of one sublattice acting on the other sublattice and H_A the anisotropy field acting on one sublattice we obtain the expression of the critical fields defined in Fig. 7:

$$\begin{cases} H_{\text{SF}} = [H_A(2H_E - H_A)]^{1/2} \\ H_C = 2H_E - H_A \text{ (paral.)} \\ H_{C'} = 2H_E + H_A \text{ (perp.)} \end{cases} \quad [3]$$

H_{SF} is the value of the antiferromagnetic to spin flop transition field extrapolated to 0 K, and H_C and $H_{C'}$ are the critical fields extrapolated to 0 K for the parallel and perpendicular cases, respectively. According to the shape of the magnetization curve reported in Fig. 8, we consider the weak anisotropy magnetization process. In randomly oriented polycrystalline materials the magnetization reaches saturation only at the highest field $H_{C'}$. From the experimental data we find $H_{\text{SF}} = 65 \pm 1 \text{ kOe}$ (Fig. 8) and $H_{C'} = 200 \pm 5 \text{ kOe}$ (Fig. 9a). The best estimation is ob-

tained with $H_E = 85 \pm 5 \text{ kOe}$ and $H_A = 30 \pm 5 \text{ kOe}$. The magnetic dipole-dipole interaction, which is important here because of the high spin state ($S = \frac{5}{2}$) and the close packing of the Fe^{3+} ions, should explain the high value of anisotropy field since no spin-orbit coupling occurs in an S ion. Each Fe^{3+} has six nearest neighbors in the layers and three next-near neighbors in each of the two adjacent layers. The exchange interaction between the layers can be expressed in terms of J_{AF} for a pair of Fe^{3+} :

$$E_{\text{exchange}} = -2J_{\text{AF}} S_1 \cdot S_2. \quad [4]$$

J_{AF} can now be determined from H_E as

$$g\mu_B H_E = 12J_{\text{AF}}S. \quad [5]$$

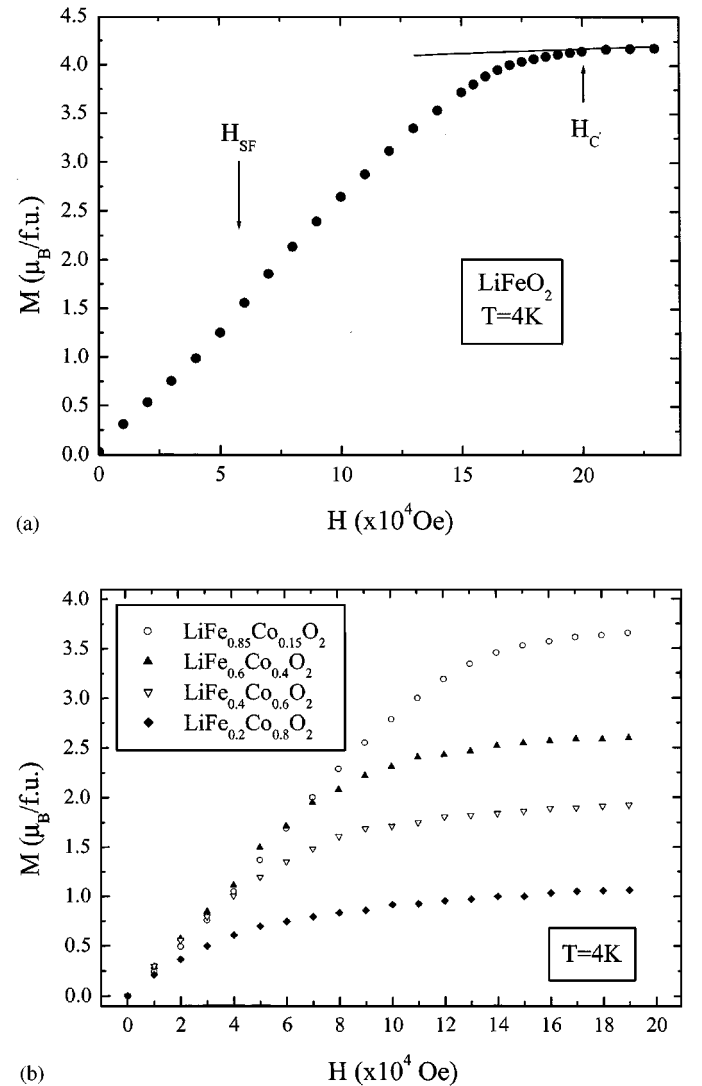


FIG. 9. Magnetic field dependence of the magnetization at 4 K for layered LiFeO_2 (a) and for $\text{LiFe}_{1-x}\text{Co}_x\text{O}_2$ with $x = 0.15, 0.4, 0.6$, and 0.8 (b). The magnetic saturation is reached for all samples.

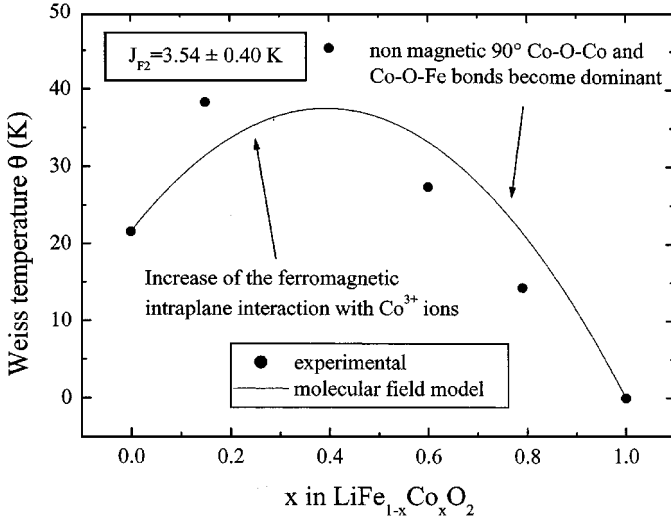


FIG. 10. Weiss temperature θ derived from high-temperature magnetization measurements ($300 \text{ K} < T < 600 \text{ K}$) as a function of x , the cobalt concentration. The continuous curve is the best fit obtained with the molecular field model given in Eq. [13].

We obtain

$$\frac{J_{\text{AF}}}{k} = -0.38 \pm 0.05 \text{ K}. \quad [6]$$

The high magnetic field measurements unambiguously confirm the high spin state of iron with $S = \frac{5}{2} (t_{2g}^3 e_g^2)$ and the low spin state of cobalt with $S = 0 (t_{2g}^6 e_g^0)$. Since the cationic disorder seems not to create ferromagnetic clusters as in $\text{Li}_{1-x}\text{Ni}_{1+x}\text{O}_2$, we can use a simple mean field model to estimate the magnetic interactions in these compounds (25). Thus we only consider Fe^{3+} and Co^{3+} ions randomly distributed in the layers. The ratio of metal ions in the lithium layers is always less than 5% in our samples and moreover we do not observe any evidence of coupling between the metal layers mediated by Fe^{3+} ion in the Li layer.

We now consider the θ Weiss values reported in Fig. 10 as a function of x . Both the increases of θ Weiss up to $x = 0.4$ and the shape of the $\theta(x)$ function suggest a direct relationship between the magnetic behaviour and the Fe–O–Co bond number. The increase of the mean ferromagnetic coupling in the Fe layers is an effect of the contraction of the a axis (Fig. 2), and particularly of the Fe(Co)–O bond due to the smaller ionic radius of low-spin Co^{3+} (0.545 Å) compared with high-spin Fe^{3+} (0.645 Å). Introducing a bigger ion like magnesium in $\text{Li}_{1-x}\text{Ni}_{1+x}\text{O}_2$ reduces immediately the θ Weiss (31), while cobalt doping increases the θ Weiss for both $\text{Li}_{1-x}\text{Ni}_{1+x}\text{O}_2$ and NaNiO_2 . In order to estimate the value of the ferromagnetic interaction within the planes, we first introduce J_{F1} and J_{AF} , the ferromagnetic intraplane

interaction between two Fe^{3+} ions and the antiferromagnetic interplane interaction, respectively. If we consider only the contraction of the Fe–O distance around the Co^{3+} ion, we can now introduce J_{F2} , the ferromagnetic intraplane interaction between two Fe^{3+} induced by the presence of Co^{3+} . We write the total magnetization using the effective chemical formula given in Table 2,

$$M_{\text{tot}} = g\mu_B (1-x) \langle S_{\text{tot}} \rangle = g\mu_B (1-x) \{ \langle S_1 \rangle + \langle S_2 \rangle \}, \quad [7]$$

where $\langle S_i \rangle$ is the average spin on sublattice i , $g = 2$ the gyromagnetic factor, and μ_B the Bohr magneton. The exchange interactions are accounted for their contributions to the local fields from the sublattice average spins as follows (in energy units):

$$\begin{cases} H_1 = g\mu_B H + 2z(1-x) \{ (1-x) J_{\text{AF}} \langle S_2 \rangle \\ \quad + [(1-x) J_{\text{F1}} + x J_{\text{F2}}] \langle S_1 \rangle \} \\ H_2 = g\mu_B H + 2z(1-x) \{ [(1-x) J_{\text{F1}} + x J_{\text{F2}}] \langle S_2 \rangle \\ \quad + (1-x) J_{\text{AF}} \langle S_1 \rangle \}. \end{cases} \quad [8]$$

Here z and H are the nearest neighbor number and the external magnetic field. The average value of the spin S_i is

$$\langle S_i \rangle = S B_S \left(\frac{S H_i}{kT} \right), \quad [9]$$

where S is the total spin number, k the Boltzmann constant, and B_S the Brillouin function. In the high-temperature limit, B_S can be approximated by

$$B_S \approx \frac{(S+1) H_i}{3kT}. \quad [10]$$

By substituting in [9] the approximation of B_S in [10] and the local field H_i given in [8], adding the two equations and solving we obtain

$$M_{\text{tot}} = g\mu_B (1-x) \langle S_{\text{tot}} \rangle = \frac{C}{T - \theta}, \quad [11]$$

where

$$C = 2 \frac{g^2 \mu_B^2 (1-x) S(S+1)}{3k} \quad [12]$$

and

$$\theta = \frac{4}{k} (1-x) [(1-x) (J_{\text{F1}} + J_{\text{AF}}) + x J_{\text{F2}}] S(S+1). \quad [13]$$

We see estimate J_{F1} by replacing the value of J_{AF} for LiFeO_2 in Eq. [13]. We find $J_{\text{F1}} = +1 \pm 0.05 \text{ K}$. The best

TABLE 2

For the Different Samples Characterized, the Following Parameters Are Reported: Lattice Constants a and c , Néel Temperature, Weiss Temperature θ , Curie Constant, Effective Moment, and Magnetization at 200 kOe

Formula	A (nm)	C (nm)	T_N (K)	θ Weiss (K)	Curie constant (J T ⁻² mol ⁻¹ K ⁻¹)	μ_{eff}/μ_B (Fe ³⁺)	M at 20 Tesla ($\mu_B/\text{f.u.}$)
LiFeO ₂	0.2961	1.457	20	+ 22	4.54	6.03	4.15
LiFe _{0.85} Co _{0.15} O ₂	0.2935	1.455	19	+ 38	3.43	5.36	3.66
LiFe _{0.6} Co _{0.4} O ₂	0.2901	1.447	8	+ 45	2.33	4.32	2.31
LiFe _{0.4} Co _{0.6} O ₂	0.2871	1.441		+ 27	1.64	3.62	1.94
LiFe _{0.2} Co _{0.8} O ₂	0.2840	1.426		+ 14	0.9	2.68	1.05
IE-LiCoO ₂	0.2814	1.404					
HT-LiCoO ₂	0.2814	1.404					

fit of the experimental values of θ for all samples using Eq. [13] then gives $J_{F2} = +3.5 \pm 0.5$ K (Fig. 10). The increase of the Weiss temperature for small doping in cobalt has already been observed in $\text{Li}_{1-x}\text{Ni}_{1+x}\text{O}_2$ and in NaNiO_2 (12, 13). We obtain positive values for both J_{F1} and J_{F2} as expected for such exchange interactions. When the number of Co ions becomes predominant ($x > 0.4$) the system tends to a paramagnet but still with short-range ferromagnetic interactions: the random distribution of iron ions in the layers leads to ferromagnetic Fe–O–Fe couplings at 90° even for low iron concentration (see Fig. 5a). Replacing all iron ions by cobalt ones leads to the diamagnetic LiCoO_2 compound (Co^{3+} in the low-spin state with $S = 0$). Assuming that at T_N a spontaneous magnetization occurs without external field gives us the expression of the Néel temperature:

$$T_N = \frac{4}{k} (1-x) [(1-x)(J_{F1} - J_{AF}) + xJ_{F2}] S(S+1). \quad [14]$$

Since the distance between successive layers of metal is of the order of 5 Å, compared with a metal–metal distance of 2.8–3 Å within the layers, the molecular field model fails especially in predicting T_N for this class of substances. The departure from the Curie–Weiss law well above T_N for all samples is actually the experimental signature of short-range order. Nevertheless, our estimated values of the exchange interactions account for the decrease of T_N with increasing x . We obtain a positive value of the Weiss temperature θ for layered LiFeO_2 as reported by Ado *et al.* and Tabuchi *et al.* (5, 16, 33). For $\alpha\text{-NaFeO}_2$ $T_N \approx 11$ K (16, 32). Following Shirane and Tabuchi (9, 17) we assume that the change of T_N between these two isomorphous compounds could be attributed to a lower interplane distance for layered LiFeO_2 . The Na^+ and Li^+ have indeed an ionic radius of 1.02 and 0.74 Å, respectively. As reported by Tabuchi *et al.* (16) ferromagnetic impurity can explain the negative θ value observed for $\alpha\text{-NaFeO}_2$ (9). We also believe that $\alpha\text{-NaFeO}_2$ and layered LiFeO_2 should have the same

magnetic structure. Neutron diffraction measurements could confirm this assumption. It is important to note the absence of frustration in layered LiFeO_2 . First, this is a good indication of a ferromagnetic interaction in the triangular Fe layers. Second, this could be correlated with the absence of ferrimagnetic clusters. A mechanism of frustration involving the clusters in LiNiO_2 has been recently proposed (12, 15). Independent of the sign of the interaction $\text{Ni(Fe)}\text{--O--Ni(Fe)}$ at 180° a Ni(Fe) ion in the Li planes tends to align the Ni(Fe) spins of the adjacent Ni(Fe) planes. This effect is in competition with the AF coupling between the Ni(Fe) layers. We have shown that the interaction involving Fe ions is not strong enough to stabilize the ferrimagnetic cluster and no frustration is in fact observed in layered LiFeO_2 . It is difficult to compare the two isomorphous systems further since in the LiNiO_2 case we cannot exclude a strong coupling between the spins and the orbital degrees of freedom (15).

IV. CONCLUSION

We have synthesized layered $\text{LiFe}_{1-x}\text{Co}_x\text{O}_2$ with $\alpha\text{-NaFeO}_2$ structure by ion-exchange reaction. In contrast to $\text{Li}_{1-x}\text{Ni}_{1+x}\text{O}_2$ we do not have any evidence of ferromagnetic clusters created by metal ions in the lithium layer and no tendency to spin frustration. We propose an A -type antiferromagnetic structure for layered LiFeO_2 with a ferromagnetic intralayer and an antiferromagnetic interlayer interaction of +1 K and –0.38 K, respectively. We show that the presence of diamagnetic cobalt ions in the iron layer induces a contraction of the Fe–O distances and thus leads to an increase in the ferromagnetic in-plane exchange interactions up to $x = 0.4$. The magnetic behavior of layered LiFeO_2 is very close to that of NaNiO_2 , even under cobalt doping. The knowledge of the magnetic coupling between Fe^{3+} ions in layered $\text{LiFe}_{1-x}\text{Co}_x\text{O}_2$ can now be used to study the behavior of other isomorphous compounds like Li(Ni, Fe)O_2 .

ACKNOWLEDGMENTS

The authors thank M. D. Núñez-Regueiro for fruitful discussions. Magnetic susceptibility measurements at high temperature were made at Laboratoire Louis Néel, CNRS France. GHMFL is a laboratory "conventionné avec l'Université Joseph Fourier de Grenoble et l'Institut National Polytechnique de Grenoble".

REFERENCES

1. C. Delmas, G. Le Flem, C. Fouassier, and P. Hagenmuller, *J. Phys. Chem. Solids* **39**, 155 (1978).
2. E. Rossen, C. D. Jones, and J. R. Dahn, *Solid State Ionics* **57**, 311 (1992).
3. T. A. Hewston and B. Chamberland, *J. Phys. Chem. Solids* **48**, 97 (1987).
4. C. Delmas, M. Ménétrier, L. Grogennec, S. Levasseur, J. P. Pères, C. Pouillier, G. Prado, L. Fournès, and F. Weill, *J. Inorg. Mater.* **1**, 11 (1999).
5. K. Ado, M. Tabuchi, H. Kobayashi, H. Kageyama, and O. Nakamura, *J. Electrochem. Soc.* **L177**, 144 (1997).
6. V. Nalbandyan and I. Sukaev, *Russ. J. Inorg. Chem. (Engl. Transl.)* **32**, 453 (1987).
7. S. Kikkawa, H. Ohkura, and M. Koizumi, *Mater. Chem. Phys.* **18**, 375 (1987).
8. B. Fuchs and S. Kemmler-Sack, *Solid State Ionics* **68**, 279 (1994).
9. T. Shirane, R. Kanno, Y. Kawamoto, Y. Takeda, M. Takano, T. Kamiyama, and F. Izumi, *Solid State Ionics* **79**, 227 (1995).
10. M. Holzapfel, A. Ott, and C. Haak, submitted.
11. A.-L. Barra, G. Chouteau, A. Stepanov, A. Rougier, and C. Delmas, *Eur. Phys. J. B* **7**, 551 (1999).
12. E. Chappel *et al.*, *Eur. Phys. J. B.* (accepted).
13. L. F. Feiner, A. M. Oles, and J. Zaanen, *Phys. Rev. Lett.* **78**, 2799 (1997).
14. Y. Kitaoka *et al.*, *J. Phys. Soc. Jpn.* **67**, 3703 (1998).
15. M. D. Núñez-Regueiro, E. Chappel, G. Chouteau, and C. Delmas, *Eur. Phys. J. B*, **16**, 37 (2000).
16. M. Tabuchi, S. Tsutsui, C. Masquelier, R. Kanno, K. Ado, I. Matsubara, S. Nasu, and H. Kageyama, *J. Solid State Chem.* **140**, 159 (1998).
17. M. Tabuchi, K. Ado, H. Kobayashi, I. Matsubara, H. Kageyama, M. Wakita, S. Tsutsui, S. Nasu, Y. Takeda, C. Masquelier, A. Hirano, and R. Kanno, *J. Solid State Chem.* **141**, 554 (1998).
18. M. Tabuchi, K. Ado, H. Kobayashi, H. Sakaebe, C. Masquelier, M. Yonemura, A. Hirano, and R. Kanno, *J. Mater. Chem.* **9**, 199 (1999).
19. P. F. Bongers and U. Enz, *Solid State Commun.* **4**, 153 (1966).
20. C. Delmas, I. Saadoune, and P. Dordor, *Mol. Cryst. Liq. Cryst.* **244**, 337 (1994).
21. I. Saadoune and C. Delmas, *J. Solid State Chem.* **136**, 8 (1998).
22. J. Rodriguez-Carjaval, *Physica B (Amsterdam)* **192**, 55 (1993).
23. R. D. Shannon, *Acta Crystallogr. A* **32**, 751 (1976).
24. A. Herpin, *Théorie du magnétisme*, PUF, Paris, 1968.
25. P. W. Anderson, *Solid State Phys.* **14**, 99 (1963).
26. J. B. Goodenough and A. L. Loeb, *Phys. Rev.* **98**, 391 (1955).
27. J. B. Goodenough, *Phys. Rev.* **100**, 564 (1955).
28. J. B. Goodenough, *J. Phys. Chem. Solids* **6**, 287 (1958).
29. J. B. Goodenough, "Magnetism and the chemical bond." Wiley Interscience, New York, 1963.
30. D. I. Khomskii and G. A. Sawatzky, *Solid State Commun.* **102**, 87 (1997).
31. C. Pouillier, L. Croguennec, C. Delmas, J. P. Perez, P. Biensan, and P. Willmann, in "Proceedings of GFECI 99, Noirmoutier, France." 1999.
32. T. Ichida, T. Shinjo, Y. Bando, and T. Takada, *J. Phys. Soc. Jpn.* **29**, 95 (1970).
33. M. Tabuchi, C. Masquelier, T. Takeuchi, K. Ado, I. Matsubara, T. Shirane, R. Kanno, S. Tsutsui, S. Nasu, H. Sakaebe, and O. Nakamura, *Solid State Ionics* **90**, 129 (1996).